Title: TRAIP is a regulator of the spindle assembly checkpoint.

Authors: Chapard C, Meraldi P, Gleich T, Bachmann D, Hohl D, Huber M

Journal: Journal of Cell Science

Year: 2014 Dec 15

Volume: 127

Issue: Pt 24

Pages: 5149-56

DOI: 10.1242/jcs.152579

The TRAF-interacting protein (TRAIP) is a regulator of the spindle assembly checkpoint

Christophe Chapard[1], Patrick Meraldi[2], Tobias Gleich[1], Daniel Bachmann[1], Daniel Hohl[1], Marcel Huber[1]

[1]Service of Dermatology, Lausanne University Hospital, Lausanne, Switzerland

[2]Department of Cell Physiology and Metabolism, University of Geneva, Geneva, Switzerland

Correspondence:
Dr. Marcel Huber
Service of Dermatology
CHUV
1011 Lausanne
Switzerland
Tel: +41-21-3140374
Fax: +41-21-3140382
Email: marcel.huber@chuv.ch

Keywords: TRAF-Interacting Protein, TRAIP, mitosis, chromosome mis-segregation, spindle assembly checkpoint

Short title: TRAIP and mitosis progression

ABSTRACT

Accurate chromosome segregation during mitosis is temporally and spatially coordinated by fidelity-monitoring checkpoint systems. Deficiencies in these checkpoint systems can lead to chromosome segregation errors and aneuploidy and promote tumorigenesis. We report that the TRAF-interacting protein (TRAIP), a ubiquitously expressed nucleolar E3 ubiquitin ligase important for cellular proliferation, was localized close to mitotic chromosomes. Its functional inactivation in HeLa cells by siRNAs decreased the time of early mitosis progression from nuclear envelope breakdown to anaphase onset and increased the percentages of chromosome alignment defects in metaphase and lagging chromosomes in anaphase compared to control cells. The decrease in progression time was corrected by the expression of wild-type but not by an ubiquitin ligase deficient form of TRAIP. TRAIP-depleted cells by-passed taxol-induced mitotic arrest, and significantly reduced kinetochore levels of MAD2 but not of other spindle checkpoint proteins in the presence of nocodazole. These results imply that TRAIP regulates the spindle assembly checkpoint, MAD2 abundance at kinetochores and the accurate cellular distribution of chromosomes. The TRAIP ubiquitin ligase activity is functionally required for the spindle assembly checkpoint control.

INTRODUCTION

The equal distribution of chromosomal DNA during mitosis is ensured by a highly complex process in which the control of APC/C (anaphase-promoting complex) activity is crucial (Foley and Kapoor, 2013; Kops et al., 2005; Pines, 2011). APC/C activity is regulated by the spindle assembly checkpoint (SAC) proteins MAD1, MAD2, BUBR1, BUB1, BUB3 and MPS1, which sense whether or not chromosomes are connected in a bi-oriented manner to opposite spindle poles through microtubules (Foley and Kapoor, 2013; Khodjakov and Pines, 2010; Santaguida and Musacchio, 2009). The strength of the SAC critically depends on the MAD2 abundance at kinetochores (Collin et al., 2013; Heinrich et al., 2013)). Defects in chromosome segregation control cause chromosomal instability and aneuploidy, common characteristics of human solid tumors (Holland and Cleveland, 2012).

Ubiquitination is a highly conserved biochemical process attaching ubiquitin monomers to proteins (Dikic et al., 2009; Welchman et al., 2005). The TRAF-interacting protein (TRAIP/TRIP/RNF206) is a RING-type E3-ubiquitin-ligase (Besse et al., 2007), but hitherto no *in vivo* substrate has been identified. Ectopically expressed TRAIP interacts with TRAF proteins and represses NF-κB signaling (Besse et al., 2007; Lee and Choi, 1997), although this might not be physiologically (Chapard et al., 2012). TRAIP is expressed ubiquitously at a low level (Lee and Choi, 1997; Su et al., 2004) in nucleoli (Zhou and Geahlen, 2009) of interphase cells but is over-expressed in breast cancer cell lines (Zhou and Geahlen, 2009) and in basal cell carcinomas (Almeida et al., 2011).

Both TRAIP knock-out mice (Park et al., 2007) and mutants of NOPO (Merkle et al., 2009), the Drosophila homolog of mammalian TRAIP, die early in development due aberrant proliferation and mitosis. TRAIP transcription is strongly down-regulated upon induction of cell cycle exit, and its knock-down decreased proliferation and caused a G1/S phase block in keratinocytes (Almeida et al., 2011). TRAIP interacts with CYLD (Regamey et al., 2003) and Syk (Zhou and Geahlen, 2009), two tumor suppressors (Bailet et al., 2009; Bignell et al., 2000; Coopman et al., 2000; Lee et al., 2005; Moroni et al., 2004), and with DNA polymerase η, which facilitates translesional synthesis after DNA damage (Wallace et al., 2014).

We report that the TRAIP protein preferentially localized around condensed chromosomes in pro- and metaphase and on chromosomal DNA from anaphase during mitosis. Its functional inactivation accelerated the progression through early phases of mitosis, reduced MAD2 recruitment to kinetochores and led to increased mitosis defects. Our findings strongly support the implication of TRAIP in SAC regulation.

RESULTS AND DISCUSSION

TRAIP preferentially localizes at the periphery of chromosomes in early mitosis

Analysis of endogenous TRAIP expression by immunofluorescence detection in mitotic cells showed localization around prometaphase and co-localization with anaphase chromosomes (Fig. 1A). To determine the specificity of the utilized antibody, immune detection of endogenous TRAIP in HeLa cells was analyzed 24h after transfection with two siRNAs targeting TRAIP (siTRAIP1 and siTRAIP2) or a scrambled negative control siRNA (siCTRL). Both TRAIP mRNA and protein levels were reduced to around 30% in TRAIP-depleted compared to control cells (Suppl. Fig. S1A). The immunofluorescence signal of endogenous TRAIP was observed in the nucleoplasm of either siCTRL- or siTRAIP-treated cells during interphase (Fig. 1B). After treatment of cells with a short detergent extraction before fixation, removing soluble proteins (Nalepa et al., 2013), the signal became nucleolar in control and disappeared in TRAIP-depleted cells. The signal in mitotic cells was localized close to congressing chromosomes in prometaphase and associated with condensed chromosomes in anaphase in control but was strongly reduced in siTRAIP- treated cells (Fig. 1C).

To validate further TRAIP localization, a lentiviral vector driving expression of a functional (Suppl. Fig. S2, (Besse et al., 2007; Zhou and Geahlen, 2009)) TRAIP-GFP was used to infect HeLa cells stably expressing α-tubulin-mRFP and H2B-CFP. In early mitotic phases cells, TRAIP-GFP dispersed throughout the cytoplasm and converged at the chromosome periphery while in later phases it co-localized with chromosomes (Fig. 1D). A small fraction accumulated during telophase in cytoplasmic particles, probably corresponding to nucleolus-derived foci (NDF) and pre-nucleolar bodies (PNB) (Dundr et al., 1997; Ma et al., 2007; Van Hooser et al., 2005).

The perichromosomal layer appears in prometaphase and disappears in telophase/cytokinesis (Hernandez-Verdun and Gautier, 1994; Ma et al., 2007; Van Hooser et al., 2005). Nucleolar proteins and RNAs bind to the surface of chromosomes at the beginning of mitosis and are incorporated again into newly formed nucleoli during telophase (Dundr et al., 1997; Van Hooser et al., 2005). Different biological functions have been assigned to chromosomal peripheral proteins (CPP) forming the perichromosomal layer (Hernandez-Verdun, 2011; Hernandez-Verdun and Gautier, 1994; Ma et al., 2007; Matsunaga and Fukui, 2010). Our analysis identified the nucleolar protein TRAIP as a CPP and prompted us to investigate TRAIP function in mitosis.

TRAIP regulates progression through early phases of mitosis

We examined the consequences of silencing TRAIP expression on mitosis duration using siRNAs and fluorescence time-lapse imaging of HeLa cells expressing H2B-EGFP and α-tubulin-mRFP (Toso et al., 2009), taking nuclear envelope breakdown (NEB) as starting time t=0min (Meraldi et al., 2004). In siCTRL-transfected cells, the median duration of mitosis was 116.7min (95% confidence interval (CI) =111.7-123.3min, range from 75 to 275min). The high variability of mitosis duration was mainly caused by the time between NEB to anaphase-onset (Lim et al., 2013; Mchedlishvili et al., 2012; Rieder et al., 1994; Toso et al., 2009) which varied from 20 to 200min (median 53.3min, 95% CI=46.7-61.7min). The time from anaphase to cytokinesis fluctuated only moderately from 45 to 85min (median 63.3min, 95% CI=60-66.7min) (Figs. 2A-D).

The average time of complete mitosis of siTRAIP1 or 2 treated cells was reduced to 96.7min (95% CI=95-101min) or 90min (95% CI=87.7-91.7min), respectively (Fig. 2A). Although the duration from anaphase to cytokinesis with siTRAIP1 (range 45 to 95min; median 66.7min, 95% CI=63.3-70min) and siTRAIP2 (range 45 to 80min; median 58.3min, 95% CI=56.7-63.3min) was very similar to control cells, the time from NEB to anaphase-onset was significantly reduced to 30min (95% CI=28.3-33.3min, range 20 to 75min) with siTRAIP1 and 26.7min (95% CI=26.7-28.3min, range 20 to 85min) with siTRAIP2 (Figs. 2B-C). Ninety percent of TRAIP-depleted cells accomplished the onset of anaphase within 45min after NEB compared to only 50% of control cells (Fig. 2E). In the skew-normal frequency distribution of anaphase-onset times, a first population (peak of the distribution) with rapid and uniform chromosome congression and a second with longer anaphase-onset times (active spindle checkpoint) can be distinguished (Meraldi et al., 2004; Rieder et al., 1994). In control siRNA-transfected HeLa cells, the skew normal distribution of anaphase-onset times had a peak (mode) at 31.8±1.2min whereas in TRAIP-depleted cells a shift to 28.4±0.4min (siTRAIP1) or 24.2±0.4min (siTRAIP2) was observed (Fig. 2F). The NEB to anaphase-onset time in cells transduced with siRNA-resistant TRAIP before siRNA transfection was indistinguishable from the control while a catalytically inactive TRAIP mutant (C25A) failed to rescue (Fig. 2G). Although MAD2 is a frequent siRNA off-target (Hubner et al., 2010; Sigoillot et al., 2012; Westhorpe et al., 2010), expression of MAD2, MAD1, BUB1 and BUB3 remained unchanged after TRAIP KD (Suppl. Fig. S1B-C). Together with the rescue data it is therefore unlikely that TRAIP KD phenotypes are caused by off-target effects. These findings suggested that the ubiquitin ligase TRAIP is implicated in the regulation of NEB to anaphase-onset time.

TRAIP loss enhances chromosome alignment defects and lagging chromosomes.

Since a reduced NEB to anaphase-onset time could induce aberrant chromosome segregation (Meraldi and Sorger, 2005; Michel et al., 2001; Perera et al., 2007), we examined whether TRAIP depletion affected chromosome behavior. The number of TRAIP-depleted cells dividing with a bipolar spindle and giving rise to two living daughter cells was not significantly different from control cells. Mitotic indexes in siRNA-treated cells were examined by anti-phospho-Histone H3(Ser28) and anti-α-tubulin immunostaining. Although mitotic indexes were comparable (Fig. 3A), the percentage of cells in prophase was reduced by 10 to 20 % in TRAIP-depleted compared to control cells (Fig. 3B), consistent with shorter NEB to anaphase-onset times. In TRAIP-depleted mitotic cells synchronized by a double-thymidine block the percentage of non-aligned chromosomes at the metaphase plate was increased compared to the control (38.5±4.9% siRNA#1, 37.1±7.6% siRNA#2, 19.6±7.5% control; mean±s.d) (Figs. 3C and E). Chromosome segregation errors were detected in mitotic cells treated with either siTRAIP1 or 2 compared to control cells (15.7±4.5% or 19.5±6.7% vs. 9.7±2.9%; mean±s.d.) (Figs. 3D and F). As expected, chromosome alignment and segregation errors were increased in MAD2-depleted cells supporting the reliability of our data (Figs. 3E-F). In summary, TRAIP down-regulation in HeLa cells leads to chromosome misalignment and segregation defects.

TRAIP loss decreases spindle assembly checkpoint function

Our results demonstrated that early mitosis and chromosome behavior are affected in response to TRAIP KD, suggesting a role of TRAIP in the SAC. To investigate whether TRAIP KD enabled HeLa cells to bypass the SAC, a taxol-induced mitotic arrest assay (Stegmeier et al., 2007a) assessing mitotic index and nuclear morphology was undertaken. CYLD and MAD2 siRNAs were used as controls for mitotic entry delay and SAC bypass (Draviam et al., 2007; Meraldi et al., 2004; Stegmeier et al., 2007a; Stegmeier et al., 2007b). Only 13±8% (mean±s.d.) of MAD2- or 51±15% of CYLD-depleted cells were mitotic (Fig. 4A-B) (Stegmeier et al., 2007b) compared to control cells (74±7%). In TRAIP depleted cells a reduced mitotic index (siRNA#1, 52±16%; siRNA#2, 53±8%) (Fig. 4B) and multilobed nuclear morphology (Stegmeier et al., 2007a; Stegmeier et al., 2007b), similarly to MAD2 siRNA treated cells (Figs. 4A and C), was found, demonstrating that loss of TRAIP led to a checkpoint-bypass phenotype. However, TRAIP depletion leads to a smaller effect than MAD2 knock-down. Whether this reflects a phenotypic difference or is due to differences in the degree of mRNA knockdown remains to be seen. Our data indicated that TRAIP depletion

was less effective compared to MAD2 knockdown (Suppl. Fig. S1A). To summarize, loss of TRAIP reduced mitotic arrest in response to the spindle poison taxol, hence led to the bypass of the SAC.

TRAIP depletion decreases Mad2 levels at unattached kinetochores.

Expression and/or localization of SAC proteins are finely modulated to regulate APC/C activity (Musacchio and Salmon, 2007) in a dose-dependent manner (Collin et al., 2013; Heinrich et al., 2013). The robustness of the SAC is in part determined by the MAD2 amount recruited to kinetochores. To elucidate whether TRAIP deficiency is affecting the kinetochore localization of SAC proteins, we performed immuno-fluorescence detection of MAD1, MAD2, BUB1, and BUBR1 proteins in TRAIP siRNA-treated cells (Fig. 4D-E). SAC proteins were correctly positioned at unattached kinetochores marked by an anti-CREST antibody in prometaphase cells. However, the amount of MAD2 recruited to the kinetochores was significantly reduced in TRAIP-depleted cells compared to control cells (70.2%±10.1% siRNA#1, 68.5%±9.9% siRNA#2, 100%±12.8% control; mean±s.d.) (Fig. 4E-F). This might be physiologically relevant since a reduction of 20% in MAD2 levels is sufficient to impair SAC activity in yeast (Heinrich et al., 2013).

In summary, we have demonstrated that TRAIP changes its predominantly nucleolar localization in interphase cells to the perichromosomal layer in mitosis. The decrease in progression time from NEB to anaphase-onset and in the binding of MAD2 to kinetochores in TRAIP-depleted cells leading to misalignment and segregation errors of chromosomes identified TRAIP as a novel regulator of SAC activity in an ubiquitin-ligase-dependent manner. Our findings most likely explain the cell death in TRAIP KO mice and NOPO mutants in Drosophila embryos since inaccurate chromosome segregation negatively impinges on the life of normal cells. The elucidation of how TRAIP functions at the molecular level to regulate the SAC awaits identification of its substrates and interaction partners.

MATERIALS AND METHODS

Cell culture

Cells were cultured in DMEM containing 10% fetal bovine serum and appropriate antibiotics (G418, 200 ug/ml; puromycin, 0.25 ug/ml). Cells were synchronized by a double-thymidine (2mM) block. Transfection of siRNAs was performed after the first thymidine treatment.

Plasmids and lentivirus

TRAIP cDNA was amplified from a human cDNA library and cloned into pEGFP-N3 (Clontech) or the lentiviral vector pCDH-CMV-MCS-EF1-Hygro (BioCat). TRAIP cDNAs with the C25A mutation or resistance to siRNAs were constructed by PCR amplification. PCR products were verified by sequencing. LV-CFP expressing H2B-CFP was purchased (Addgene #25998). Cells were infected (MOI of 10) with lentivirus (Almeida et al., 2011) and selected with 800ug/ml hygromycin.

Protein extractions and TRAIP auto-ubiquitination

Proteins were extracted by cell lysis in 1% SDS/phosphate-buffered saline. For immunoblots the following antibodies were used: GFP (Clontech), actin (Sigma), rabbit-anti-TRAIP (Abcam), goat-anti-TRAIP antibody (Imgenex), MAD2 (Covance) and HA (Santa Cruz Biotechnology). TRAIP auto-ubiquitination was carried out as described (Almeida et al., 2008). Signals from immunoblots were captured by LAS4000 (GE) and analysed by ImageJ.

RNA interference

siRNA targeting human TRAIP mRNA (NM_005879.2) and Control siRNA (Origene), hCYLD (Draviam et al., 2007; Sun et al., 2010), and hMAD2 (Uzunova et al., 2012) were transfected into cells at 30nM final concentration using INTERFERin (Polyplus).

Live-cell imaging and immunofluorescence analysis

Experiments were performed at 37°C/5%CO_2 in cell culture chambers (MatTek) in phenol red-free medium. For time-lapse experiments 24h after siRNA transfection, images were recorded every 5 min for 16h using a 20x Plan-NeofluarNA0.5 objective on a Axio Observer.Z1 microscope (Zeiss). Confocal live-cell imaging experiments were performed using 63x/1.40 oil objective on a LSM700 confocal laser scanning microscope (Zeiss). The following antibodies were used for immunofluorescence: GFP (Clontech), TRAIP (Abcam),

phospho-Histone-H3(Ser28) (Cell Signaling Technology), tubulin (Sigma), nucleolin C23 (Santa Cruz Biotechnology), MAD1 (Meraldi et al., 2004), MAD2 (Bethyl Laboratories), BUB1 (Klebig et al., 2009), BUBR1 (Klebig et al., 2009), and CREST (Klebig et al., 2009). Images were analyzed using ImageJ. Kinetochore MAD2 levels were quantified as described (McClelland et al., 2007).

Taxol assay

The taxol assay inHeLa cells was carried out as described (Stegmeier et al., 2007a) except for DNA staining with Dapi. MosaiX images were acquired using 20xobjective on a Axio Imager microscope (Zeiss) equipped with DIC and Dapi filters. Cells were scored using ImageJ.

RNA isolation and qRT-PCR analysis

RNA was purified using RNeasy Kit (Qiagen) and cDNA was synthesized using Primescript-RT Kit (TakaRa). Quantitative PCR analysis was performed (Almeida et al., 2011) using RPL13A (endogenous reference), TRAIP, CYLD, MAD1, Bub1B, Bub3 (Qiagen) or MAD2 (Universal Probe Library, Roche) primers.

Statistical analyses

Statistical significance, denoted as * $p<0.05$, ** $p<0.01$, *** $p<0.001$,**** $p<0.0001$, was calculated using 1way-ANOVA followed by Tukey's multiple comparisons test or 2way-ANOVA followed by Tukey-Kramer's Post Hoc test (GraphPad Prism6).

ACKNOWLEDGEMENTS

We thank Dr. Elaine Fuchs for LV-CFP plasmid (Nat Med 16, 821 (2010)), Dr. Didier Trono for psPAX2 and pMD2.G plasmids (J Virol 77, 8957 (2003)) and Florence Morgenthaler from the Cellular Imaging Facility, Lausanne University. MH is supported by the Swiss National Science Foundation (Grant 31003A-138416) and the Emma Muschamp Foundation. PM acknowledges support from the Swiss National Science Foundation (Grant 31003A-141256), the University of Geneva and the Louis-Jeantet Foundation. MH designed and supervised the present study. CC, TG and DB performed experiments. CC, PM, DH and MH wrote and discussed the paper.

CONFLICT OF INTEREST

The authors declare no interest of conflict.

References

Almeida S., Maillard C., Itin P., Hohl D., and Huber M. (2008). Five new CYLD mutations in skin appendage tumors and evidence that aspartic acid 681 in CYLD is essential for deubiquitinase activity. *J. Invest. Dermatol.* **128**, 587-593.

Almeida S., Ryser S., Obarzanek-Fojt M., Hohl D., and Huber M. (2011). The TRAF-Interacting Protein (TRIP) Is a Regulator of Keratinocyte Proliferation. *J. Invest. Dermatol.* **131**, 349-357.

Bailet O., Fenouille N., Abbe P., Robert G., Rocchi S., Gonthier N., Denoyelle C., Ticchioni M., Ortonne J. P., Ballotti R., Deckert M., and Tartare-Deckert S. (2009). Spleen tyrosine kinase functions as a tumor suppressor in melanoma cells by inducing senescence-like growth arrest. *Cancer Res.* **69**, 2748-2756.

Besse A., Campos A. D., Webster W. K., and Darnay B. G. (2007). TRAF-interacting protein (TRIP) is a RING-dependent ubiquitin ligase. *Biochem. Biophys. Res. Commun.* **359**, 660-664.

Bignell G. R., Warren W., Seal S., Takahashi M., Rapley E., Barfoot R., Green H., Brown C., Biggs P. J., Lakhani S. R., Jones C., Hansen J., Blair E., Hofmann B., Siebert R., Turner G., Evans D. G., Schrander-Stumpel C., Beemer F. A., van Den Ouweland A., Halley D., Delpech B., Cleveland M. G., Leigh I., Leisti J., and Rasmussen S. (2000). Identification of the familial cylindromatosis tumour-suppressor gene. *Nat. Genet.* **25**, 160-165.

Chapard C., Hohl D., and Huber M. (2012). The role of the TRAF-interacting protein in proliferation and differentiation. *Exp. Dermatol.* **21**, 321-326.

Collin P., Nashchekina O., Walker R., and Pines J. (2013). The spindle assembly checkpoint works like a rheostat rather than a toggle switch. *Nat. Cell Biol.* **15**, 1378-1385.

Coopman P. J., Do M. T., Barth M., Bowden E. T., Hayes A. J., Basyuk E., Blancato J. K., Vezza P. R., McLeskey S. W., Mangeat P. H., and Mueller S. C. (2000). The Syk tyrosine kinase suppresses malignant growth of human breast cancer cells. *Nature* **406**, 742-747.

Dikic I., Wakatsuki S., and Walters K. J. (2009). Ubiquitin-binding domains - from structures to functions. *Nat. Rev. Mol. Cell. Biol.* **10**, 659-671.

Draviam V. M., Stegmeier F., Nalepa G., Sowa M. E., Chen J., Liang A., Hannon G. J., Sorger P. K., Harper J. W., and Elledge S. J. (2007). A functional genomic screen

identifies a role for TAO1 kinase in spindle-checkpoint signalling. *Nat. Cell Biol.* **9**, 556-564.

Dundr M., Meier U. T., Lewis N., Rekosh D., Hammarskjold M. L., and Olson M. O. (1997). A class of nonribosomal nucleolar components is located in chromosome periphery and in nucleolus-derived foci during anaphase and telophase. *Chromosoma* **105**, 407-417.

Foley E. A., and Kapoor T. M. (2013). Microtubule attachment and spindle assembly checkpoint signalling at the kinetochore. *Nat. Rev. Mol. Cell. Biol.* **14**, 25-37.

Heinrich S., Geissen E. M., Kamenz J., Trautmann S., Widmer C., Drewe P., Knop M., Radde N., Hasenauer J., and Hauf S. (2013). Determinants of robustness in spindle assembly checkpoint signalling. *Nat. Cell Biol.* **15**, 1328-1339.

Hernandez-Verdun D. (2011). Assembly and disassembly of the nucleolus during the cell cycle. *Nucleus* **2**, 189-194.

Hernandez-Verdun D., and Gautier T. (1994). The chromosome periphery during mitosis. *Bioessays* **16**, 179-185.

Holland A. J., and Cleveland D. W. (2012). Losing balance: the origin and impact of aneuploidy in cancer. *EMBO Rep.* **13**, 501-514.

Hubner N. C., Wang L. H., Kaulich M., Descombes P., Poser I., and Nigg E. A. (2010). Re-examination of siRNA specificity questions role of PICH and Tao1 in the spindle checkpoint and identifies Mad2 as a sensitive target for small RNAs. *Chromosoma* **119**, 149-165.

Khodjakov A., and Pines J. (2010). Centromere tension: a divisive issue. *Nat. Cell Biol.* **12**, 919-923.

Klebig C., Korinth D., and Meraldi P. (2009). Bub1 regulates chromosome segregation in a kinetochore-independent manner. *J. Cell Biol.* **185**, 841-858.

Kops G. J., Weaver B. A., and Cleveland D. W. (2005). On the road to cancer: aneuploidy and the mitotic checkpoint. *Nat. Rev. Cancer* **5**, 773-785.

Lee D. A., Grossman M. E., Schneiderman P., and Celebi J. T. (2005). Genetics of skin appendage neoplasms and related syndromes. *J. Med. Genet.* **42**, 811-819.

Lee S. Y., and Choi Y. (1997). TRAF-interacting protein (TRIP): a novel component of the tumor necrosis factor receptor (TNFR)- and CD30-TRAF signaling complexes that inhibits TRAF2-mediated NF-kappaB activation. *J. Exp. Med.* **185**, 1275-1285.

Lim S., Kawamura E., Fielding A. B., Maydan M., and Dedhar S. (2013). Integrin-Linked Kinase Regulates Interphase and Mitotic Microtubule Dynamics. *PloS One* **8**, e53702.

Ma N., Matsunaga S., Takata H., Ono-Maniwa R., Uchiyama S., and Fukui K. (2007). Nucleolin functions in nucleolus formation and chromosome congression. *J. Cell Sci.* **120**, 2091-2105.

Matsunaga S., and Fukui K. (2010). The chromosome peripheral proteins play an active role in chromosome dynamics. *BioMolecular Concepts* **1**, 157-164.

McClelland S. E., Borusu S., Amaro A. C., Winter J. R., Belwal M., McAinsh A. D., and Meraldi P. (2007). The CENP-A NAC/CAD kinetochore complex controls chromosome congression and spindle bipolarity. *EMBO J.* **26**, 5033-5047.

Mchedlishvili N., Wieser S., Holtackers R., Mouysset J., Belwal M., Amaro A. C., and Meraldi P. (2012). Kinetochores accelerate centrosome separation to ensure faithful chromosome segregation. *J. Cell Sci.* **125**, 906-918.

Meraldi P., Draviam V. M., and Sorger P. K. (2004). Timing and checkpoints in the regulation of mitotic progression. *Dev. Cell* **7**, 45-60.

Meraldi P., and Sorger P. K. (2005). A dual role for Bub1 in the spindle checkpoint and chromosome congression. *EMBO J.* **24**, 1621-1633.

Merkle J. A., Rickmyre J. L., Garg A., Loggins E. B., Jodoin J. N., Lee E., Wu L. P., and Lee L. A. (2009). no poles encodes a predicted E3 ubiquitin ligase required for early embryonic development of Drosophila. *Development* **136**, 449-459.

Michel L. S., Liberal V., Chatterjee A., Kirchwegger R., Pasche B., Gerald W., Dobles M., Sorger P. K., Murty V. V., and Benezra R. (2001). MAD2 haplo-insufficiency causes premature anaphase and chromosome instability in mammalian cells. *Nature* **409**, 355-359.

Moroni M., Soldatenkov V., Zhang L., Zhang Y., Stoica G., Gehan E., Rashidi B., Singh B., Ozdemirli M., and Mueller S. C. (2004). Progressive loss of Syk and abnormal proliferation in breast cancer cells. *Cancer Res.* **64**, 7346-7354.

Musacchio A., and Salmon E. D. (2007). The spindle-assembly checkpoint in space and time. *Nat. Rev. Mol. Cell. Biol.* **8**, 379-393.

Nalepa G., Barnholtz-Sloan J., Enzor R., Dey D., He Y., Gehlhausen J. R., Lehmann A. S., Park S. J., Yang Y., Yang X., Chen S., Guan X., Chen Y., Renbarger J., Yang F. C., Parada L. F., and Clapp W. (2013). The tumor suppressor CDKN3 controls mitosis. *J. Cell Biol.* **201**, 997-1012.

Park E. S., Choi S., Kim J. M., Jeong Y., Choe J., Park C. S., Choi Y., and Rho J. (2007). Early embryonic lethality caused by targeted disruption of the TRAF-interacting protein (TRIP) gene. *Biochem. Biophys. Res. Commun.* **363**, 971-977.

Perera D., Tilston V., Hopwood J. A., Barchi M., Boot-Handford R. P., and Taylor S. S. (2007). Bub1 maintains centromeric cohesion by activation of the spindle checkpoint. *Dev. Cell* **13**, 566-579.

Pines J. (2011). Cubism and the cell cycle: the many faces of the APC/C. *Nat. Rev. Mol. Cell. Biol.* **12**, 427-438.

Regamey A., Hohl D., Liu J. W., Roger T., Kogerman P., Toftgard R., and Huber M. (2003). The tumor suppressor CYLD interacts with TRIP and regulates negatively nuclear factor kappaB activation by tumor necrosis factor. *J. Exp. Med.* **198**, 1959-1964.

Rieder C. L., Schultz A., Cole R., and Sluder G. (1994). Anaphase onset in vertebrate somatic cells is controlled by a checkpoint that monitors sister kinetochore attachment to the spindle. *J. Cell Biol.* **127**, 1301-1310.

Santaguida S., and Musacchio A. (2009). The life and miracles of kinetochores. *EMBO J.* **28**, 2511-2531.

Sigoillot F. D., Lyman S., Huckins J. F., Adamson B., Chung E., Quattrochi B., and King R. W. (2012). A bioinformatics method identifies prominent off-targeted transcripts in RNAi screens. *Nat. Meth.* **9**, 363-366.

Stegmeier F., Rape M., Draviam V. M., Nalepa G., Sowa M. E., Ang X. L., McDonald E. R., 3rd, Li M. Z., Hannon G. J., Sorger P. K., Kirschner M. W., Harper J. W., and Elledge S. J. (2007a). Anaphase initiation is regulated by antagonistic ubiquitination and deubiquitination activities. *Nature* **446**, 876-881.

Stegmeier F., Sowa M. E., Nalepa G., Gygi S. P., Harper J. W., and Elledge S. J. (2007b). The tumor suppressor CYLD regulates entry into mitosis. *Proc. Natl. Acad. Sci. U S A* **104**, 8869-8874.

Su A. I., Wiltshire T., Batalov S., Lapp H., Ching K. A., Block D., Zhang J., Soden R., Hayakawa M., Kreiman G., Cooke M. P., Walker J. R., and Hogenesch J. B. (2004). A gene atlas of the mouse and human protein-encoding transcriptomes. *Proc. Natl. Acad. Sci. U S A* **101**, 6062-6067.

Sun L., Gao J., Huo L., Sun X., Shi X., Liu M., Li D., Zhang C., and Zhou J. (2010). Tumour suppressor CYLD is a negative regulator of the mitotic kinase Aurora-B. *J. Pathol.* **221**, 425-432.

Toso A., Winter J. R., Garrod A. J., Amaro A. C., Meraldi P., and McAinsh A. D. (2009). Kinetochore-generated pushing forces separate centrosomes during bipolar spindle assembly. *J. Cell Biol.* **184**, 365-372.

Uzunova K., Dye B. T., Schutz H., Ladurner R., Petzold G., Toyoda Y., Jarvis M. A., Brown N. G., Poser I., Novatchkova M., Mechtler K., Hyman A. A., Stark H., Schulman B. A., and Peters J. M. (2012). APC15 mediates CDC20 autoubiquitylation by APC/C(MCC) and disassembly of the mitotic checkpoint complex. *Nat. Struct. Mol. Biol.* **19**, 1116-1123.

Van Hooser A. A., Yuh P., and Heald R. (2005). The perichromosomal layer. *Chromosoma* **114**, 377-388.

Wallace H. A., Merkle J. A., Yu M. C., Berg T. G., Lee E., Bosco G., and Lee L. A. (2014). TRIP/NOPO E3 ubiquitin ligase promotes ubiquitylation of DNA polymerase eta. *Development* **141**, 1332-1341.

Welchman R. L., Gordon C., and Mayer R. J. (2005). Ubiquitin and ubiquitin-like proteins as multifunctional signals. *Nat. Rev. Mol. Cell. Biol.* **6**, 599-609.

Westhorpe F. G., Diez M. A., Gurden M. D., Tighe A., and Taylor S. S. (2010). Re-evaluating the role of Tao1 in the spindle checkpoint. *Chromosoma* **119**, 371-379.

Zhou Q., and Geahlen R. L. (2009). The protein-tyrosine kinase Syk interacts with TRAF-interacting protein TRIP in breast epithelial cells. *Oncogene* **28**, 1348-1356.

Figure Legends

Fig. 1: Endogenous and ectopic TRAIP is a chromosomal peripheral protein during mitosis. (A) Confocal images of mitotic HeLa cells immuno-stained with anti-TRAIP antibody (green). (B-C) Confocal images of HeLa cells in interphase (B) or mitosis (C) immuno-stained for endogenous TRAIP (red) and α-tubulin (green) 24h after treatment with the indicated siRNAs. Extraction was carried out with 0.1% Triton X-100 for 2 min before fixation (B). The settings for confocal imaging were identical within experiments. Scale bar = 5μm. DNA was marked with Dapi (blue). (D) Confocal images of living HeLa cells stably expressing α-tubulin-mRFP (red), H2B-CFP (blue) together with TRAIP-GFP (green). PNB and NDF are marked by grey and white arrowheads, respectively. Scale bars = 5μm.

Fig. 2: TRAIP depletion decreased the NEB to anaphase time. (A-C) Scatter plot (median with inter-quartile range) of times for full mitosis (A), NEB to anaphase onset (B), anaphase onset to cytokinesis (C) in siRNA-treated HeLa cells. N=3 independent experiments, n=225 cells. (D) Successive frames from live-cell movies. Scale bar = 5μm. (E) Cumulative frequency plots of anaphase-onset times with NEB=0 min. (N=3, n=225). (F) Frequency distribution of anaphase-onset times (N=3, n=225). (G) Rescue of the decreased NEB to anaphase-onset time by the expression of siRNA-resistant wild-type but not by catalytically inactive (ci, C25A) TRAIP. Median with inter-quartile range; N=3, n=180.

Fig. 3: TRAIP depletion leads to chromosome alignment defects and lagging chromosomes. (A) Mitotic index of siRNA-treated HeLa cells (N=3, n=7000) (B) Distribution of siRNA-treated HeLa cells in the different phases of mitosis (N=3, n=250). (C-D) Representative images of siRNA-transfected HeLa cells in metaphase (C) and anaphase (D). Arrows show unaligned (C) or lagging chromosomes (D). Scale bar = 5μm. (E) Fraction of cells with unaligned chromosomes at metaphase plate (N=3, n>100, for siCTRL, siTRAIP1 and siTRAIP2; N=2, n=14 (siMAD2) and 60 (siCYLD). (F) Fraction of cells with segregation errors in anaphase (N=3, n>150, for siCTRL, siTRAIP1 and siTRAIP2; N=2, n=69 (siMAD2) and 45 (siCYLD). Results in (A-B) are shown as mean±s.e.m.

Fig. 4: TRAIP regulates the spindle checkpoint by reducing MAD2 at unattached kinetochores. (A) Representative images of siRNA-transfected HeLa cells treated with 100 nM taxol for 24 hours. Scale bar = 30μm. (B-C) The percentage of mitotic cells (B) and cells

with either multilobed or interphase nuclei (C) was counted by cell rounding in DIC microscopy and Dapi staining. Results are represented as mean±s.e.m. (N=4, n>2700, for siCTRL, siTRAIP1 and siTRAIP2; N=2, n=400 for siMAD2 and siCYLD). (D-E) Confocal images of siRNA-treated HeLa cells immuno-stained for CREST (red), and either MAD1, MAD2, BUB1 (green) or BUBR1 (purple). Cells in (E) were treated with nocodazole (1µg/ml) for 1h prior to analysis. Scale bar = 5µm. (F) Scatter plot of MAD2 intensities at single kinetochores in nocodazole-treated cells shown in (E). Quantification of MAD2 levels relative to the CREST signal (median with inter-quartile range). The total mean signal for MAD2 in control cells was normalised to 1.

Supplementary Figures

Supplementary Figure S1: RNA interference in HeLa cells. Analysis of mRNA (A-C) and protein (A-B) levels were analyzed by quantitative PCR and immunoblot 24h after siRNA-transfection of HeLa cells. Results are reported as representative mean±s.d. of 2 or more independent experiments.

Supplementary Figure S2: TRAIP-GFP is a functional fusion protein. (A) Western blot of TRAIP-GFP (IB: TRAIP) and HA-ubiquitin (IB: HA) after immunoprecipitation of TRAIP-GFP from 293T cells transfected with pCMV-TRAIPGFP and/or pHA-Ub. B) Confocal images of cells after immuno-staining for GFP (green) and nucleolin (red). Scale bar = 10μm.

Figure1

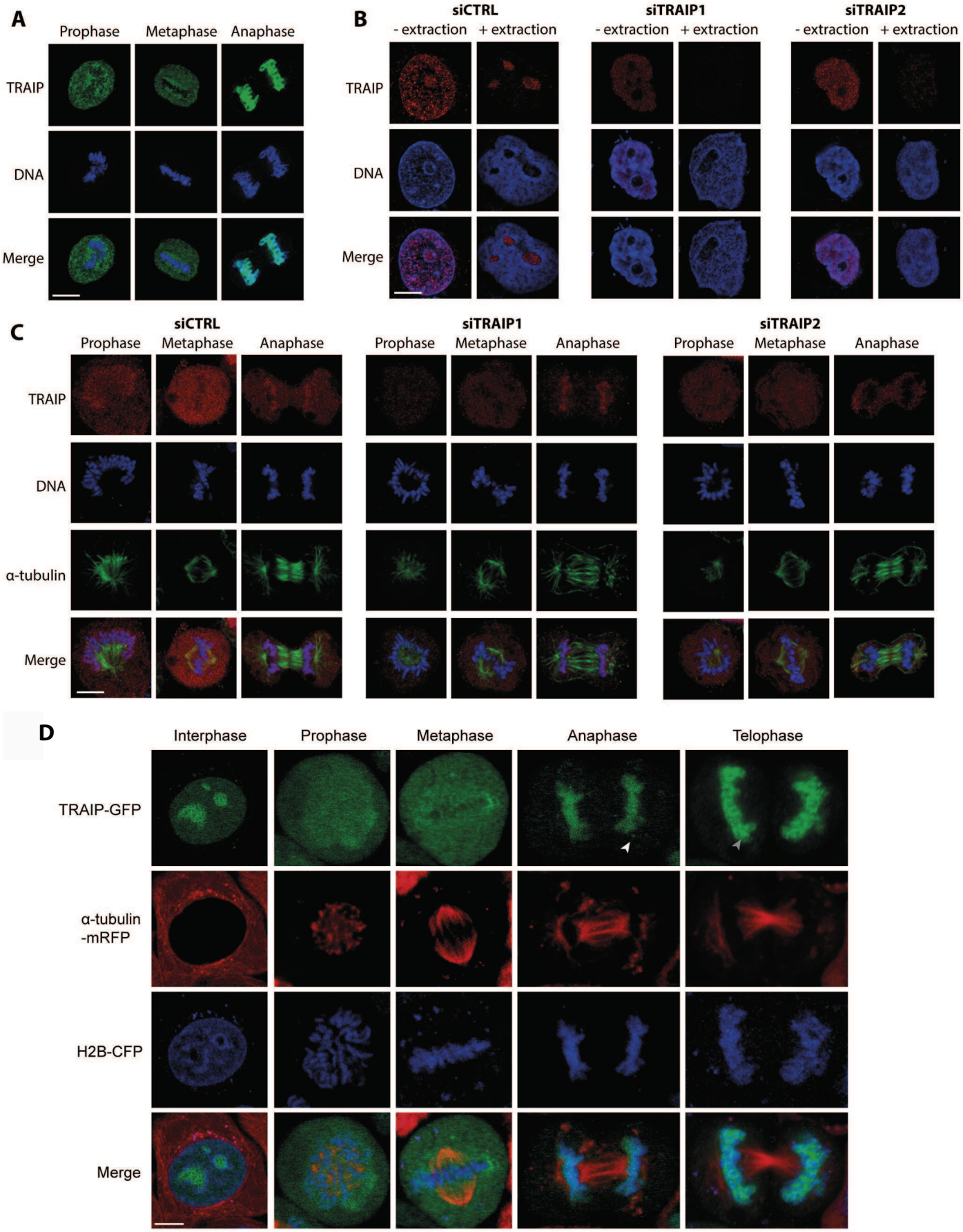
A
Prophase
Metaphase
Anaphase
TRAIP
DNA
Merge
B
siCTRL
siTRAIP1
siTRAIP2
- extraction
+ extraction
TRAIP
DNA
Merge
C
siCTRL
siTRAIP1
siTRAIP2
Prophase
Metaphase
Anaphase
TRAIP
DNA
α-tubulin
Merge
D
Interphase
Prophase
Metaphase
Anaphase
Telophase
TRAIP-GFP
α-tubulin
-mRFP
H2B-CFP
Merge

Figure 2

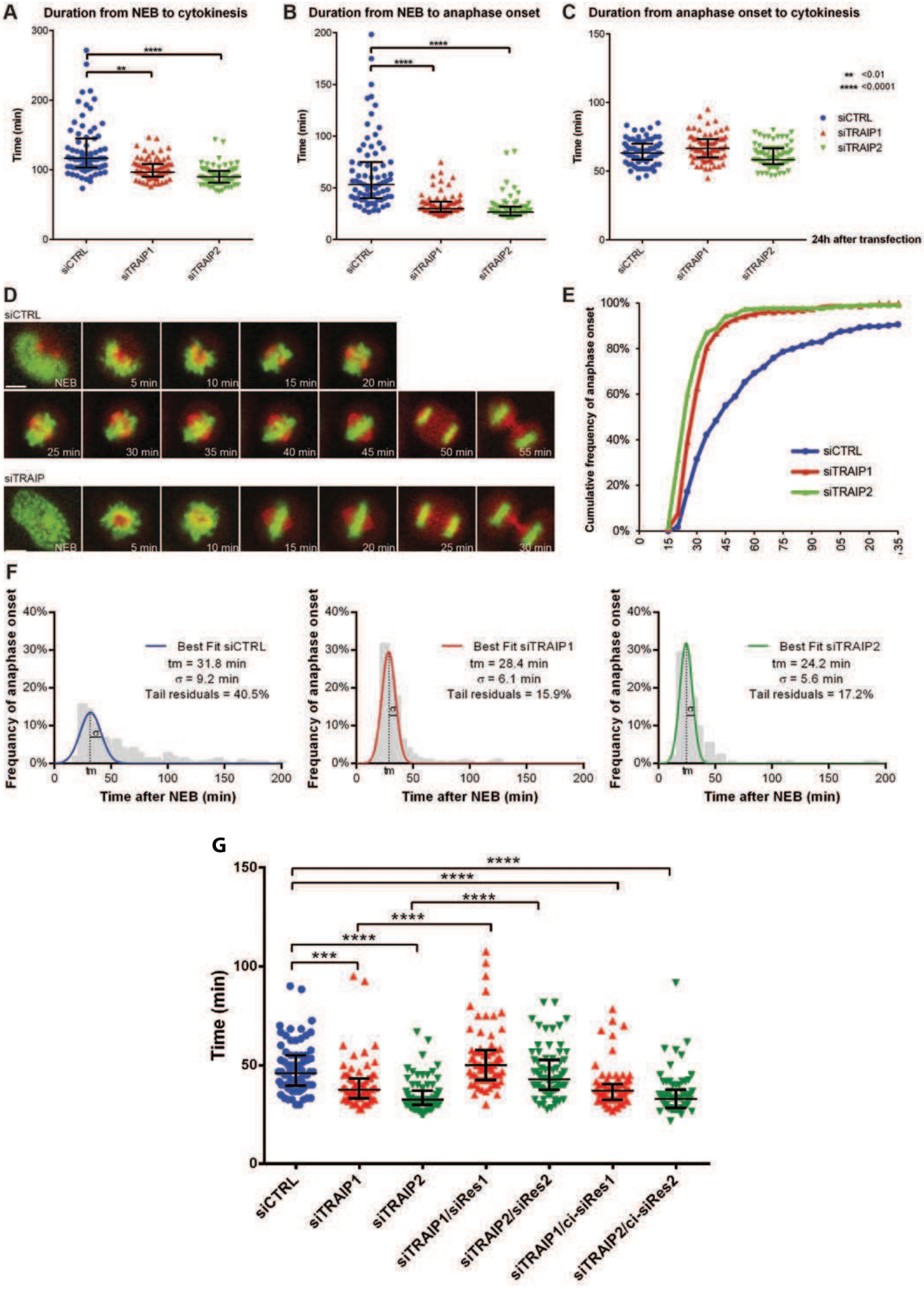
A
Duration from NEB to cytokinesis
Time (min)
siCTRL
siTRAIP1
siTRAIP2
B
Duration from NEB to anaphase onset
C
Duration from anaphase onset to cytokinesis
** <0.01
**** <0.0001
24h after transfection
D
siCTRL
siTRAIP
NEB
5 min
10 min
15 min
20 min
25 min
30 min
35 min
40 min
45 min
50 min
55 min
E
Cumulative frequency of anaphase onset
F
Frequancy of anaphase onset
Best Fit siCTRL
tm = 31.8 min
σ = 9.2 min
Tail residuals = 40.5%
Best Fit siTRAIP1
tm = 28.4 min
σ = 6.1 min
Tail residuals = 15.9%
Best Fit siTRAIP2
tm = 24.2 min
σ = 5.6 min
Tail residuals = 17.2%
Time after NEB (min)
G
siTRAIP1/siRes1
siTRAIP2/siRes2
siTRAIP1/ci-siRes1
siTRAIP2/ci-siRes2

Figure 3

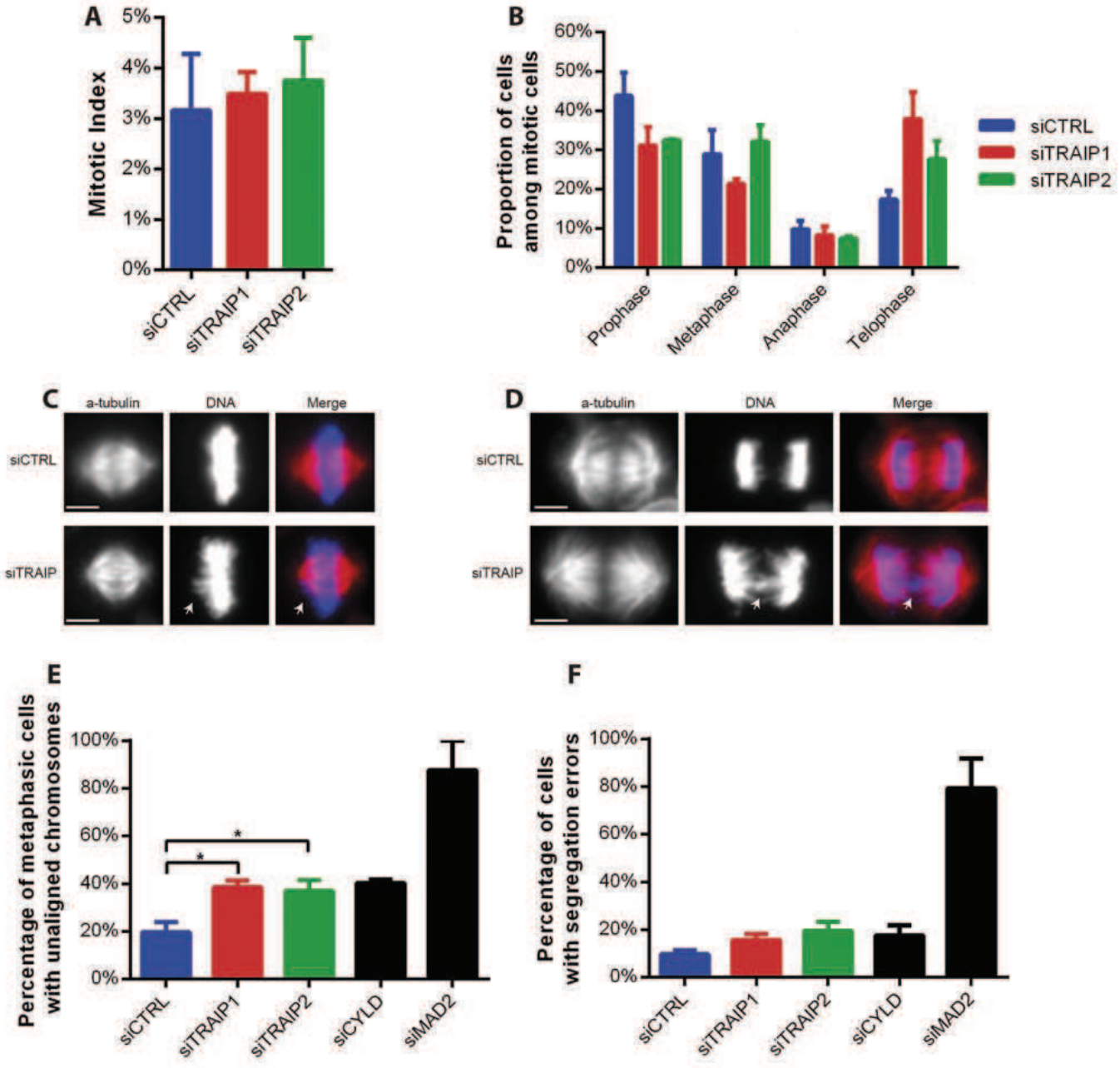
A
Mitotic Index
5%
4%
3%
2%
1%
0%
siCTRL
siTRAIP1
siTRAIP2
B
Proportion of cells among mitotic cells
60%
50%
40%
30%
20%
10%
0%
Prophase
Metaphase
Anaphase
Telophase
siCTRL
siTRAIP1
siTRAIP2
C
a-tubulin
DNA
Merge
siCTRL
siTRAIP
D
a-tubulin
DNA
Merge
siCTRL
siTRAIP
E
Percentage of metaphasic cells with unaligned chromosomes
100%
80%
60%
40%
20%
0%
*
*
siCTRL
siTRAIP1
siTRAIP2
siCYLD
siMAD2
F
Percentage of cells with segregation errors
100%
80%
60%
40%
20%
0%
siCTRL
siTRAIP1
siTRAIP2
siCYLD
siMAD2

Figure 4

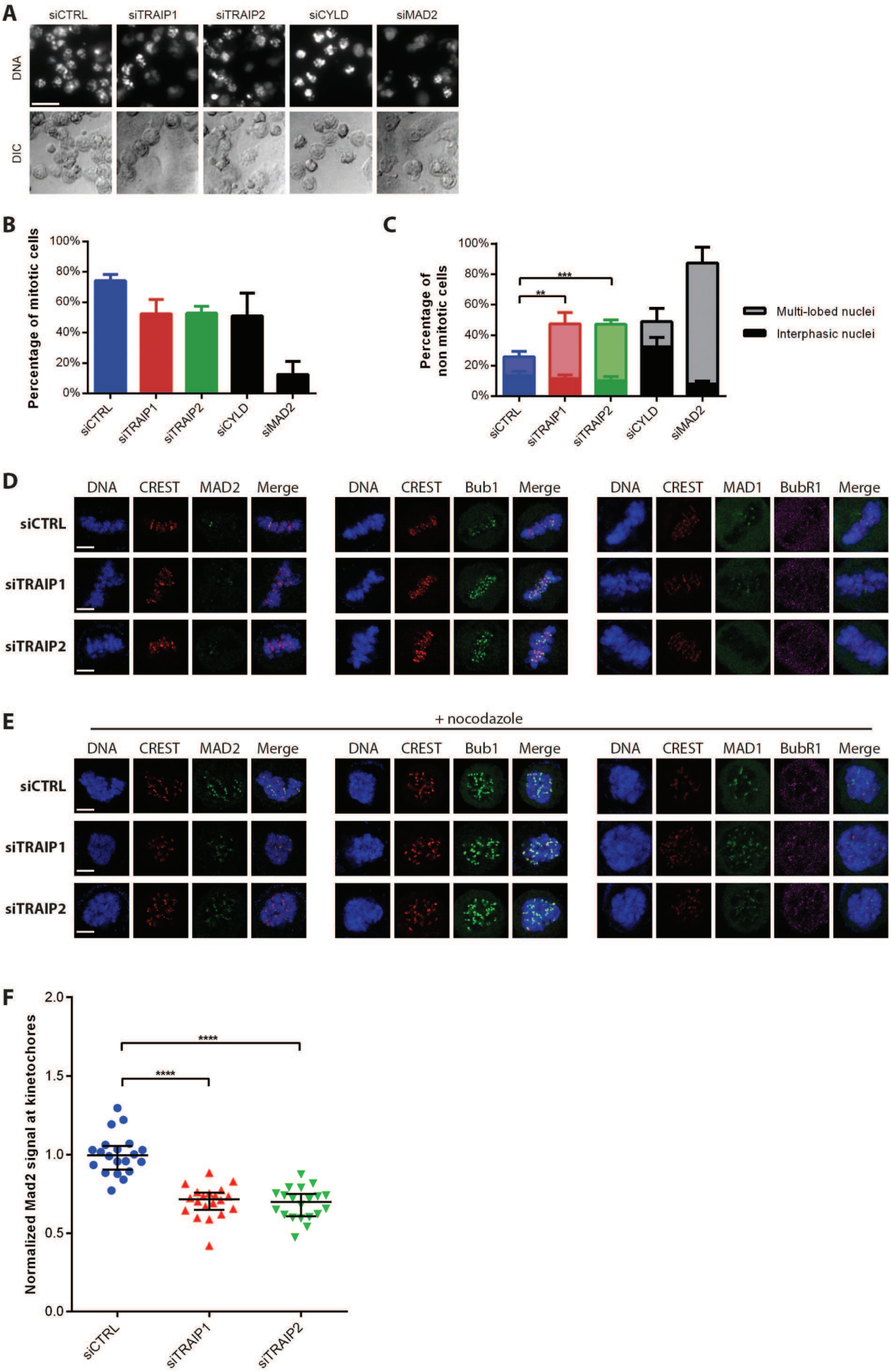
A
siCTRL
siTRAIP1
siTRAIP2
siCYLD
siMAD2
DNA
DIC
B
Percentage of mitotic cells
100%
80%
60%
40%
20%
0%
siCTRL
siTRAIP1
siTRAIP2
siCYLD
siMAD2
C
Percentage of non mitotic cells
***
**
Multi-lobed nuclei
Interphasic nuclei
D
DNA
CREST
MAD2
Merge
Bub1
MAD1
BubR1
siCTRL
siTRAIP1
siTRAIP2
E
+ nocodazole
F
Normalized Mad2 signal at kinetochores
2.0
1.5
1.0
0.5
0.0
****
****

Suppl. Figure S1

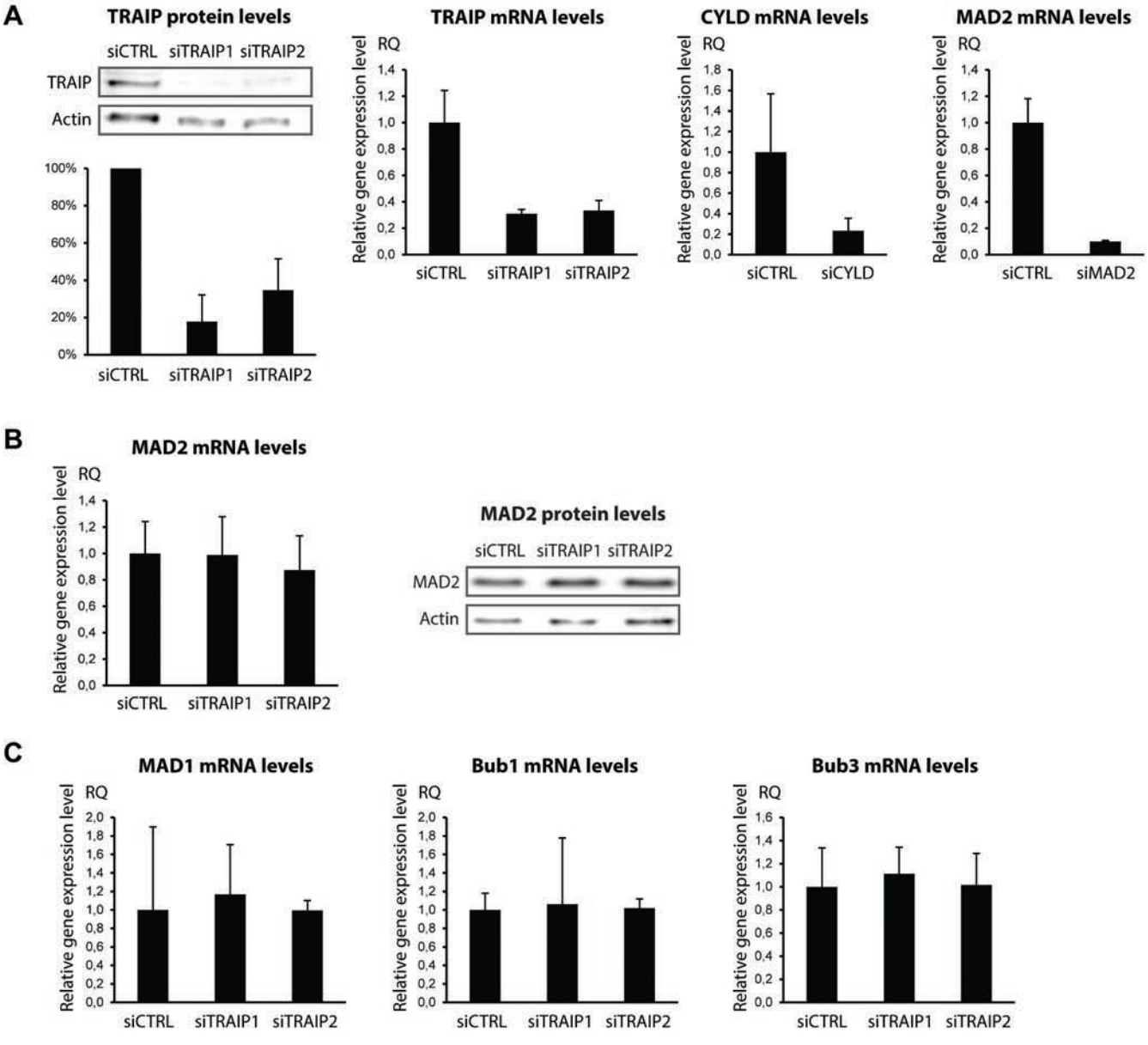

Suppl. Figure S2